Prediction of Rate Constants for Combustion and Pyrolysis Reactions by Bimolecular QRRK

Bimolecular QRRK (Quantum Rice-Ramsperger-Kassel) analysis is a simple method for calculating rate constants of addition and recombination reactions, based on unimolecular quantum-RRK theory. Input parameters are readily derived, and rate constants and reaction branching can be predicted with remarkable accuracy. Such predictive power makes the method especially useful in developing mechanisms of elementary reactions. Furthermore, from the bimolecular QRRK equations, limiting forms of the rate constants in the limits of low and high pressure are developed. Addition/stabilization is pressure-dependent at low pressure but pressure-independent at high pressure, as is conventionally understood for simple decomposition, its reverse. In distinct contrast, addition with chemically activated decomposition has the opposite behavior: pressure independence at low pressure and pressure dependence [as (pressure)$^{-1}$] at high pressure. The method is tested against data and illustrated by calculations for $O + CO \rightarrow CO_2$; for $H + O_2 \rightarrow HO_2$ or $O + OH$; for $H + C_2H_4 \rightarrow C_2H_5$ or $C_2H_3 + H_2$; and for $H + C_2H_3 \rightarrow C_2H_4$ or $H_2 + C_2H_2$.

P. R. Westmoreland, J. B. Howard and J. P. Longwell
Department of Chemical Engineering,
Massachusetts Institute of Technology
Cambridge, MA 02139

A. M. Dean
Exxon Research and Engineering
Annandale, NJ 08801

Introduction

Decomposition of a radical or molecule has a unimolecular, pressure-independent rate constant in the limit of high pressure, but as pressure is reduced the rate constant eventually decreases with pressure. In the low-pressure limit, it becomes directly proportional to pressure. The pressures at which the transition or falloff region occurs are strong functions of temperature, so at a given pressure the rate constant can have pronounced non-Arrhenius behavior. Rationalizing and quantifying these effects, first accomplished in the 1920's, again has become an active area of research (Robinson and Holbrook, 1972; Forst, 1973; Troe, 1977; Pritchard, 1984).

Radical combination or radical-molecule addition would seem to be simply the reverse of decomposition, having the same falloff behavior by microscopic reversibility. This is true for the specific reaction channel that gives formation of the collisionally stabilized adduct. The reason is that the adduct species has an energy distribution in thermal equilibrium with the surrounding gas molecules, just as for a species that is thermally decomposing.

However, it is very important but not so well recognized that additional products can be formed from combination and addition reactions by chemically activated pathways. The initially formed adduct has a chemical activation energy distribution, different from a thermal energy distribution because the thermal energies of the reactants are augmented by the chemical energy released by making the new bond. This chemical energy is the same as the energy barrier for redissociation of the collisionally stabilized adduct to the original adducts. If the energy in the chemical activation energy distribution extends above the barrier for a new dissociation (or an isomerization) of the adduct, then that reaction pathway can also occur.

Calculations of the bimolecular rate constant involve the concept that the fate of the chemically activated adduct is determined by competition among the possible pathways: stabilization by collisions, redissociation to reactants, or formation of new products by dissociation or isomerization. RRKM methods have been applied only for a few reactions (e.g., Berman and Lin, 1983), partly because of the complexity of the analysis and

Correspondence concerning this paper should be addressed to P.R. Westmoreland, Department of Chemical Engineering, University of Massachusetts, Amherst, MA 01003.

partly because of the transition state parameters that are needed.

Bimolecular QRRK analysis has been proposed (Dean, 1985) as a less sophisticated but more easily used method for analyzing such problems. In the present paper, the rate constants of chemically activated decompositions are shown to be pressure-independent at low pressure but pressure-dependent at high pressure, which is the inverse of our normal concept of falloff. Furthermore, the accuracy of this method is tested successfully for four representative sets of combustion and pyrolysis reactions that have well-measured rate constants: $O(^3P) + CO \rightarrow CO_2$; $H + O_2 \rightarrow HO_2$ or $O + OH$; $H + C_2H_4 \rightarrow C_2H_5$ or $C_2H_3 + H_2$; and $H + C_2H_3 \rightarrow C_2H_4$ or $H_2 + C_2H_2$. No input parameters were adjusted.

Unimolecular QRRK Equations

Dean (1985) has presented equations for bimolecular rate constants based on the quantum-RRK or QRRK unimolecular reaction theory of Kassel (1928), which treats the storage of excess energy (relative to the ground state) as quantized vibrational energy. The concepts and several of the terms of the equations are taken from unimolecular QRRK.

In the simplest form of the theory, the assumption is made that the s vibrations of the decomposing molecule can be represented by a single frequency ν, usually a geometric mean $\langle\nu\rangle$ of the molecule's frequencies (Robinson and Holbrook, 1972). Next, each energy E is divided into $E/h\langle\nu\rangle$ vibrational quanta. For the energy variable E, the symbol n is used, and for the energy barrier to reaction E_o, the quantized energy is m quanta; quantum levels and the rate processes are illustrated in Figure 1a. The apparent k_{uni}:

$$k_{uni} = \frac{1}{[A]} \cdot \frac{d[\text{Products}]}{dt} \tag{1}$$

then is evaluated by a sum over all energies, assuming pseudo-steady state for each energy level of A^* and collisional excitation or deexcitation with rate constants k_{exc} and k_{deexc}:

$$k_{uni} = \frac{1}{[A]} \sum_{\substack{E=E_o \\ (n=m)}}^{\infty} k_{rxn}(E) \cdot [A^*(E)]$$

$$= \sum_{\substack{E=E_o \\ (n=m)}}^{\infty} k_{rxn}(E) \cdot \frac{k_{deexc}[M] \cdot K(E,T)}{k_{deexc}[M] + k_{rxn}(E)} \tag{2}$$

where $K(E,T)$ is the thermal-energy distribution function (k_{exc}/k_{deexc}) and M is an unspecified third-body species. Kassel assumed that if a molecule were excited to an energy E, then $k_{rxn}(E)$ would be proportional to the probability that one of the s oscillators could have energy E_o or greater (sufficient energy to cause reaction); that is, m or more of the n total quanta. The proportionality constant was shown to be $\mathcal{A}_\infty$, the Arrhenius preexponential factor for dissociation of A in the high-pressure limit, so the energy-dependent rate constant is:

$$k_{rxn}(E) = \mathcal{A}_\infty \cdot \frac{n!(n-m+s-1)!}{(n-m)!(n+s-1)!} \tag{3}$$

Likewise, he derived the quantized thermal energy distribution

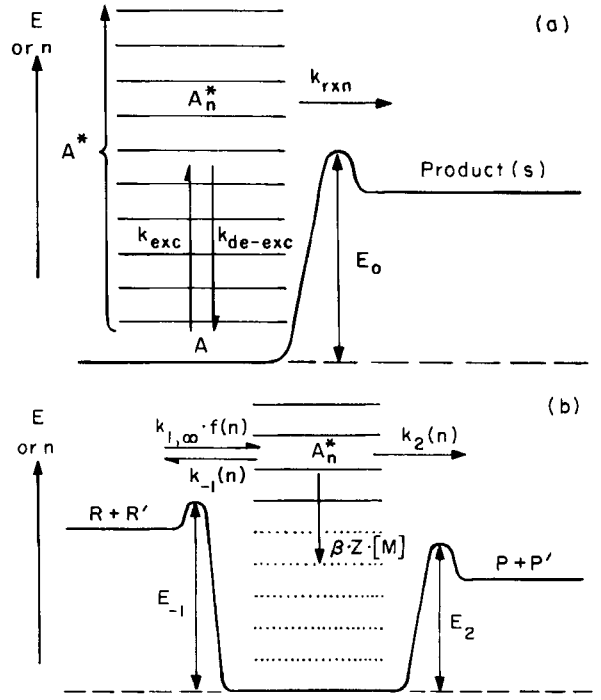

Figure 1. Energy diagrams for pressure-dependent reactions.

a. Unimolecular reaction
b. Bimolecular reaction with chemically activated pathway

$K(E,T)$ to be:

$$K(E,T) = \alpha^n \cdot (1-\alpha)^s \frac{(n+s-1)!}{n!(s-1)!} \tag{4}$$

where $\alpha = \exp(-h\langle\nu\rangle/\kappa T)$.

In the present development, a collisional efficiency β has been applied to modify the traditional but incorrect strong-collision assumption that $k_{deexc} = Z \cdot [M]$, where Z is the collision frequency rate constant. The strong-collision assumption implies that any collision between A^* and M would have to remove all the excess energy from A^*. Note that any species included as M would have to accommodate this energy content, regardless of its capacity for accepting the energy. Analyzing collisional energy transfer by master-equation methods, Troe (1977) fit most of the temperature dependence of β with the equation:

$$\frac{\beta}{1-(\beta)^{1/2}} = \frac{-\langle\Delta E_{coll}\rangle}{F(E) \cdot \kappa T} \tag{5}$$

where $\langle\Delta E_{coll}\rangle$ is the average amount of energy transferred per collision and $F(E)$ is a factor, weakly dependent on energy, that is related to the number of excited states. Over the temperature range of 300–2,500 K for a series of reactions (Troe, 1977), $F(E) = 1.15$ was a median value. The value of β depends on the specific third-body molecule M through the value of $\langle\Delta E_{coll}\rangle$.

Bimolecular QRRK Equations

The bimolecular QRRK equations follow (Dean, 1985) from unimolecular QRRK and the definition of the chemical activation distribution function. Consider the general case of addition

to form an excited adduct A^*, followed by stabilization, redissociation to reactants, or chemically activated decomposition:

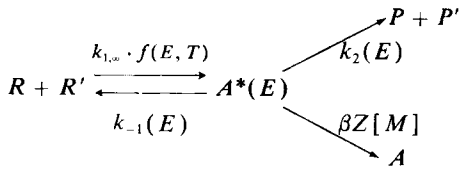

Here, $k_{1,\infty}$ is the high-pressure-limit rate constant for forming adduct and $f(E, T)$ is the energy distribution for chemical activation (after Robinson and Holbrook, 1972):

$$f(E,T) = \frac{k_{-1}(E) \cdot K(E,T)}{\sum\limits_{\substack{E-E_{-1} \\ (n=m_{-1})}}^{\infty} k_{-1}(E) \cdot K(E,T)} \tag{6}$$

where $K(E, T)$ is the QRRK thermal distribution from Eq. 4. Rate constants $k_{-1}(E)$ and $k_2(E)$ are calculated from the QRRK equation for $k_{rxn}(E)$ (Eq. 3) using $m_{-1}\,(E_{-1}/h\langle\nu\rangle)$ and $m_2\,(E_2/h\langle\nu\rangle)$, respectively. A typical energy diagram for these reactions is shown in Figure 1b.

To obtain the bimolecular rate constant for a particular product channel, a pseudosteady-state analysis is made as before. The rate constant for forming the addition/stabilization product A from $R + R'$ is:

$$k_{a/s} = \sum_{\substack{E-E_{-1} \\ (n=m_{-1})}}^{\infty} \beta Z[M] \cdot \frac{k_{1,\infty} \cdot f(E,T)}{\beta Z[M] + k_{-1}(E) + k_2(E)} \tag{7}$$

and, for forming the addition/decomposition products P and P':

$$k_{a/d} = \sum_{\substack{E-E_{-1} \\ (n=m_{-1})}}^{\infty} k_2(E) \cdot \frac{k_{1,\infty} \cdot f(E,T)}{\beta Z[M] + k_{-1}(E) + k_2(E)} \tag{8}$$

If more decomposition channels are available, the $k_{rxn}(E)$ for each channel is added in the denominator of Eqs. 7 and 8, and an equation in the form of Eq. 8 is written for each additional channel, substituting the respective $k_{rxn}(E)$ for $k_2(E)$ as the multiplier term.

Low- and High-Pressure Limits

The low-pressure and high-pressure limits for these channels may be derived from Eqs. 7 and 8. As pressure changes, the rate constants change because of the relative magnitudes of terms in the denominator, $\beta Z[M]$ vs. $k_{-1}(E)$ and $k_2(E)$.

The low-pressure limit for addition/stabilization (or recombination) is derived from Eq. 7 to be

$$\lim_{[M] \to 0} k_{a/s} = [M] \cdot \sum_{\substack{E-E_{-1} \\ (n=m_{-1})}}^{\infty} \beta Z \cdot \frac{k_{1,\infty} \cdot f(E,T)}{k_{-1}(E) + k_2(E)}, \tag{9}$$

sometimes written as $[M] \cdot k_o$ (as a termolecular reaction), and the high-pressure limit reduces properly to $k_{1,\infty}$. At a given temperature, the falloff curve for stabilization can be plotted as $\log(k_{a/s})$ vs. $\log(P)$ or $\log([M])$.

Note the presence of $k_2(E)$ in Eq. 9. If chemically activated conversion of A^* is more rapid than decomposition to reactants $[k_2(E) \gg k_{-1}(E)]$, then Eq. 9 shows that $k_{o,a/s}$ will be dominated by $k_2(E)$ rather than by $k_{-1}(E)$. Thus, ignoring the chemically activated pathway could give incorrect rate constants for "simple" addition.

Similar analysis of Eq. 8 implies that chemically activated decomposition has a falloff curve that is the opposite of addition/stabilization, with a rate constant that is pressure-independent at low pressure and inversely proportional to pressure at high pressure. From Eq. 8, the low-pressure limit for the chemically activated pathway to P and P' will be

$$\lim_{[M] \to 0} k_{a/d} = k_{1,\infty} \cdot \sum_{\substack{E-E_{-1} \\ (n=m_{-1})}}^{\infty} \frac{k_2(E) \cdot f(E,T)}{k_{-1}(E) + k_2(E)} \tag{10}$$

and the high-pressure limit will be

$$\lim_{[M] \to \infty} k_{a/d} = \frac{1}{[M]} \cdot \frac{k_{1,\infty}}{\beta Z} \cdot \sum_{\substack{E-E_{-1} \\ (n=m_{-1})}}^{\infty} k_2(E) \cdot f(E,T) \tag{11}$$

with an inverse pressure dependence. While this result goes against past intuition about low- and high-pressure limits, it is a natural consequence of physics when chemically activated reactions are recognized as possibilities. Accordingly, the same type of behavior will result from RRKM equations. One consequence is that a reaction of the form $A + B \rightarrow C + D$ with a rate constant measured to be pressure-independent may be proceeding via addition.

Any bimolecular process that forms an excited adduct can potentially have pressure-dependent or pressure-independent rate constants and branching. In contrast are the rate constants for H-atom metathetical reactions (such as $CH_4 + OH \rightarrow CH_3 + H_2O$), which would not be affected by pressure. By the description of Benson (1976), the adduct in such a reaction would be a single transition state $(CH_3 \cdot H \cdot OH)^{\ddagger}$ with one-electron half-bonds, not a chemical species that could be stabilized.

Sources of Input Data

Predictions by this method can be made quickly, in part because the input data are few and frequently are easy to obtain:

- Preexponential factors and activation energies in the high-pressure limit, $\mathcal{A}_\infty$ and $E_{act,\infty}$.
- The number of vibrational degrees of freedom for the adduct, s ($3 \cdot n_{atoms} - 5$ for linear molecules, $3 \cdot n_{atoms} - 6$ for nonlinear).
- The geometric mean of the adduct's vibrational frequencies, $\langle\nu\rangle$.
- Lennard-Jones transport properties, σ and ϵ/κ, for the adduct and for the third-body gas.
- The average energy transferred per collision with the third-body gas, $\langle\Delta E_{coll}\rangle$, which has been experimentally evaluated for a variety of gases.

Obtaining $\mathcal{A}_\infty$ and $E_{act,\infty}$ may be the most difficult task. These parameters can come from literature data, from estimates by the methods of Benson (1976, 1983), from the generic rate con-

stants of Dean (1985), or from the equilibrium constant and the reverse rate constant (high-pressure limit).

Lennard-Jones collisional properties (Reid et al., 1977; Kee et al., 1983) for the stabilized species A and the third-body gas M are used to calculate a collision rate constant Z_{LJ}. Establishing the $\langle \Delta E_{coll} \rangle$ needed to calculate collisional efficiency β (from Eq. 5) is an active area of research, but several compilations are available (Troe, 1979; Gardiner and Troe, 1984; Cobos et al., 1985b).

Ambiguities in these parameters cause some uncertainty in the predictions. For example, the QRRK $k_{rxn}(E)$ equation, Eq. 3, contains the assumption that $\mathcal{A}_\infty$ and $E_{act,\infty}$ are independent of temperature, but they may not be. Also, the vibrational degrees of freedom include internal rotations, which can have very low frequencies when approximated by harmonic oscillators; the values chosen for those frequencies dramatically affect $\langle \nu \rangle$. Further, the assignment of all excess energy to vibrational energy can be inexact when there are significant changes in angular momentum. Finally, using a single geometric-mean $\langle \nu \rangle$ to represent all the ν's in a molecule may be too great an approximation. Use of the arithmetic mean has been suggested to improve the predictions (Thiele et al., 1980).

Tests of Bimolecular QRRK

Bimolecular QRRK is remarkably effective in predicting the pressure-dependent rate constants of many combustion and pyrolysis reactions. Four detailed applications show how parameters are selected and what results can be obtained. Fundamental oxidation reactions (O + CO and H + O_2) and H + hydrocarbon reactions (H + C_2H_4 and H + C_2H_3) were chosen.

Reaction of O + CO

Destruction of CO by O is important in the dry combustion of CO and because of the puzzling non-Arrhenius behavior of its rate constant. It is unimportant for hydrocarbon combustion, where OH is formed, because destruction of CO by OH is much faster. For example, at 2,000 K and 1 atm (101.3 kPa), k_{OH} is $5 \cdot 10^{11}\ s^{-1}$, while $k_{O\text{-atom}}$ is $1 \cdot 10^{9}\ s^{-1}$ (Warnatz, 1984). In fact, a major problem in accurately measuring the rate constant for O + CO has been that any H_2O impurity leads to OH, which accelerates CO destruction significantly (Baulch et al., 1976).

Available data on the reaction (Baulch et al., 1976; Warnatz, 1984) are treated as third-order (O + CO + M $\rightarrow$ CO_2 + M) with rate constant k_o). The puzzle is that the data, despite scatter, seem to show a positive E_{act} at low temperatures but negative E_{act} at high temperatures. This switch seems to occur at about 1,000 K. As a consequence, Baulch et al. recommended k_o only for the range 250–500 K, while Warnatz recommended k_o only for 1,000–3,000 K.

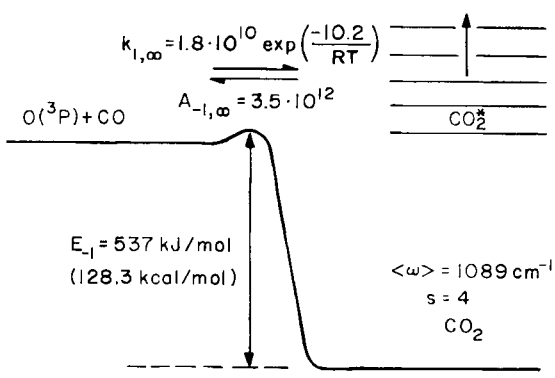

Figure 2. Energy diagram for $O(^3P)$ + CO $\rightarrow$ CO_2.
Units: mol, cm, s, kJ

It is simple to obtain the parameters for this bimolecular QRRK analysis, which are shown in the energy diagram of Figure 2. Experimental Arrhenius parameters $\mathcal{A}_\infty$ and $E_{act,\infty}$ for addition are cited by Troe (1974). For the dissociation, $\mathcal{A}_{-1,\infty}$ and E_{-1} are calculated by detailed balancing using the equilibrium constant at 298 K. The number of vibrational degrees of freedom s for CO_2 is four, and the geometric mean frequency $\langle \omega \rangle$ of 1,089 cm^{-1} was calculated from CO_2 frequencies listed in the JANAF tables (Stull et al., 1972). Lennard-Jones parameters σ and ϵ/κ for CO_2 and for M = Ar were taken from Kee et al. (1983). From Troe (1979), the average energy transferred per collision for Ar was chosen as $\langle \Delta E_{coll} \rangle$ = 3.4 kJ/mol (0.80 kcal/mol).

The analysis showed good agreement with the data, including the maximum in the rate constant. In Figure 3, recent measurements made in Ar are taken from a recent review (Warnatz, 1984). In comparison to these data, predictions are shown of k_o and of $k_{bi}/[M]$ at 100 kPa (1 atm). Agreement is quite good, especially considering that no parameters were adjusted and that not all measurements were experimentally confirmed to be in the low-pressure limit. Most notably, the prediction resolves the apparent inconsistency between the low- and high-temperature data by showing a maximum near 1,000 K.

The reasons for the maximum also can be established from QRRK components of k_o. Equation 9 for $k_{o,a/s}$ may be rewritten in this case [$k_2(E) = 0$] as

$$k_{o,a/s} = \sum_{\substack{E=E_1 \\ (n=n_1)}}^{\infty} \frac{k_{1,\infty} \cdot \beta Z}{k_{-1}(E)} \cdot f(E, T). \qquad (12)$$

In effect, the energy distribution function $f(E, T)$ is a weighting function for a ratio that has a temperature-dependent numerator and an energy-dependent denominator, Table 1.

The maximum in k_o can be explained by examining the energy and temperature dependences of this weighting function, numerator, and denominator. At a given energy level, the ratio

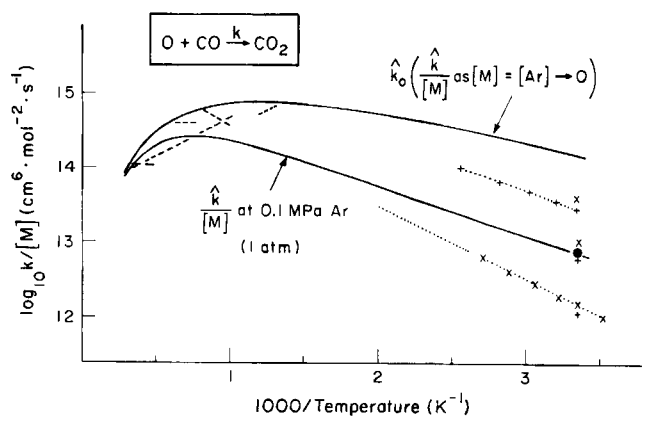

Figure 3. Comparison of rate constants of $O(^3P)$ + CO $\rightarrow$ CO_2.
— QRRK predictions
x, +, ---, ····· Data of Warnatz (1984)

Table 1. Components of Rate Constant for $O(^3P) + CO \rightarrow CO_2$ in Low-Pressure Limit k_0*

		Temperature, K									
		300		500		1,000		1,500		2,000	
		Log_{10} (Numerator, $k_{1,\infty} \cdot \beta \cdot Z_{LJ}$)									
		22.59		23.20		23.58		23.65		23.67	
Quantum Level vs. $m_{-1} = 41$	Log_{10} [Denominator $k_{-1}(E)$]	$f(E)$	Log_{10} (Num/Den)	$f(E)$	Log_{10} (Num/Den)	$f(E)$	Log_{10} (Num/Den)	$f(E)$	Log_{10} (Num/Den)	$f(E)$	Log_{10} (Num/Den)
0 (at E_{-1})	8.42	0.98	14.16	0.84	14.78	0.39	15.16	0.18	15.23	0.087	15.25
1	8.99	0.021	13.59	0.15	14.21	0.33	14.59	0.25	14.66	0.16	14.68
2	9.36	—	—	0.016	13.84	0.17	14.22	0.22	14.29	0.18	14.31
3	9.64	—	—	—	—	0.071	13.95	0.15	14.02	0.17	14.03
4	9.85	—	—	—	—	0.026	13.73	0.095	13.81	0.13	13.82
5	10.03	—	—	—	—	—	—	0.053	13.63	0.097	13.64
6	10.18	—	—	—	—	—	—	0.028	13.48	0.066	13.49
7	10.30	—	—	—	—	—	—	—	—	0.043	13.36
8	10.42	—	—	—	—	—	—	—	—	0.027	13.25
$\text{Log}_{10}(k_o)$	—		14.15		14.72		14.86		14.69		14.48

*Sum over energy of (Numerator/Denominator) · $f(E, T)$ as shown in Eq. 12.
Units: cm, mol, s

increases with temperature (because of the numerator) by an order of magnitude from 300 to 1,000 K, but it increases only slightly from 1,000 to 2,000 K. At a given temperature, the ratio increases sharply with increasing energy (because of the denominator) in the lower quantum levels. There would be no maximum if only a single energy of CO_2^* were involved, but $f(E, T)$ emphasizes the higher energy levels more as temperature increases. Thus, at low temperatures, the lowest energy state dominates, causing k_o to increase with increasing temperature as if there were only one energy; while at higher temperatures, the shift in $f(E, T)$ toward the higher energy levels and the weak temperature dependence of the numerator cause k_o to drop with increasing temperature.

Reactions of H + O_2 and O + OH

Destruction of O_2 by H-atom, which is one of the most important reactions in combustion, leads to two different sets of products. A common misconception is that there are two reactions, one dependent on pressure and forming HO_2, the other independent of pressure and forming O + OH. In fact, there are two pathways from the same addition process, as HO_2^* is formed and can be stabilized or can decompose.

These pathways are both important. When HO_2 is formed, reactive H is scavenged from the system. The second, chain-branching pathway forms two highly reactive radicals, O and OH, which themselves have important roles in combustion, including the regeneration of H from reactions with H_2, H_2O, and CO. Modeling of combustion is also sensitive to the reaction of O + OH to form H + O_2, and thermal decomposition of HO_2 can be significant in ignition (Warnatz, 1984). Consequently, all these rate constants have been studied extensively by experiment and theory.

The broad data base for these reactions make them good test cases for the bimolecular QRRK method. Parameters are shown in the energy diagram of Figure 4. For O + OH $\rightarrow$ HO_2, k_∞ was estimated by modifying Benson's method for recombination of alkyl radicals (Benson, 1983; Westmoreland, 1986). The k_∞ for H + $O_2 \rightarrow$ HO_2 was taken from Cobos et al. (1985a), and Arrhenius parameters for the reverse reactions were calculated using equilibrium constants at 298 K. All thermodynamic data were taken from the JANAF tables (Stull et al., 1972) except for $\Delta H^0_{f,298}(HO_2)$ = 10.5 kJ/mol (2.5 kcal/mol) (Howard, 1980). The geometric mean frequency $\langle\omega\rangle$ for HO_2 is calculated to be 1,734 cm^{-1} (Stull et al., 1972) with s = 3 oscillators. For $\langle\Delta E_{coll}\rangle$ of H_2, 2.6 kJ/mol (0.61 kcal/mol) was used (Troe, 1979).

Predictions of the rate constants are remarkably good, as shown in Figure 5. Rate constants for the chain-branching reaction H + $O_2 \rightarrow$ O + OH, Figure 5a, vary only slightly within the scatter of data. At elevated pressures, this reaction could

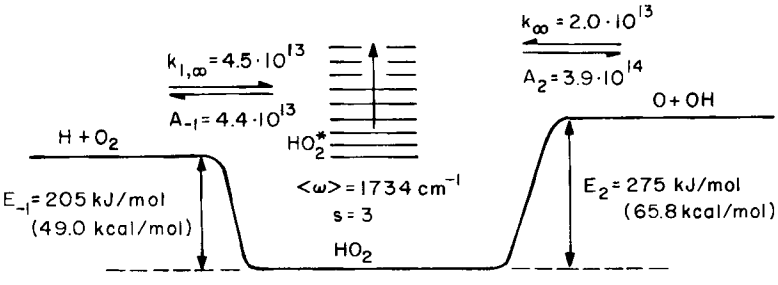

Figure 4. Energy diagram for H + O_2/HO_2/$O(^3P)$ + OH.

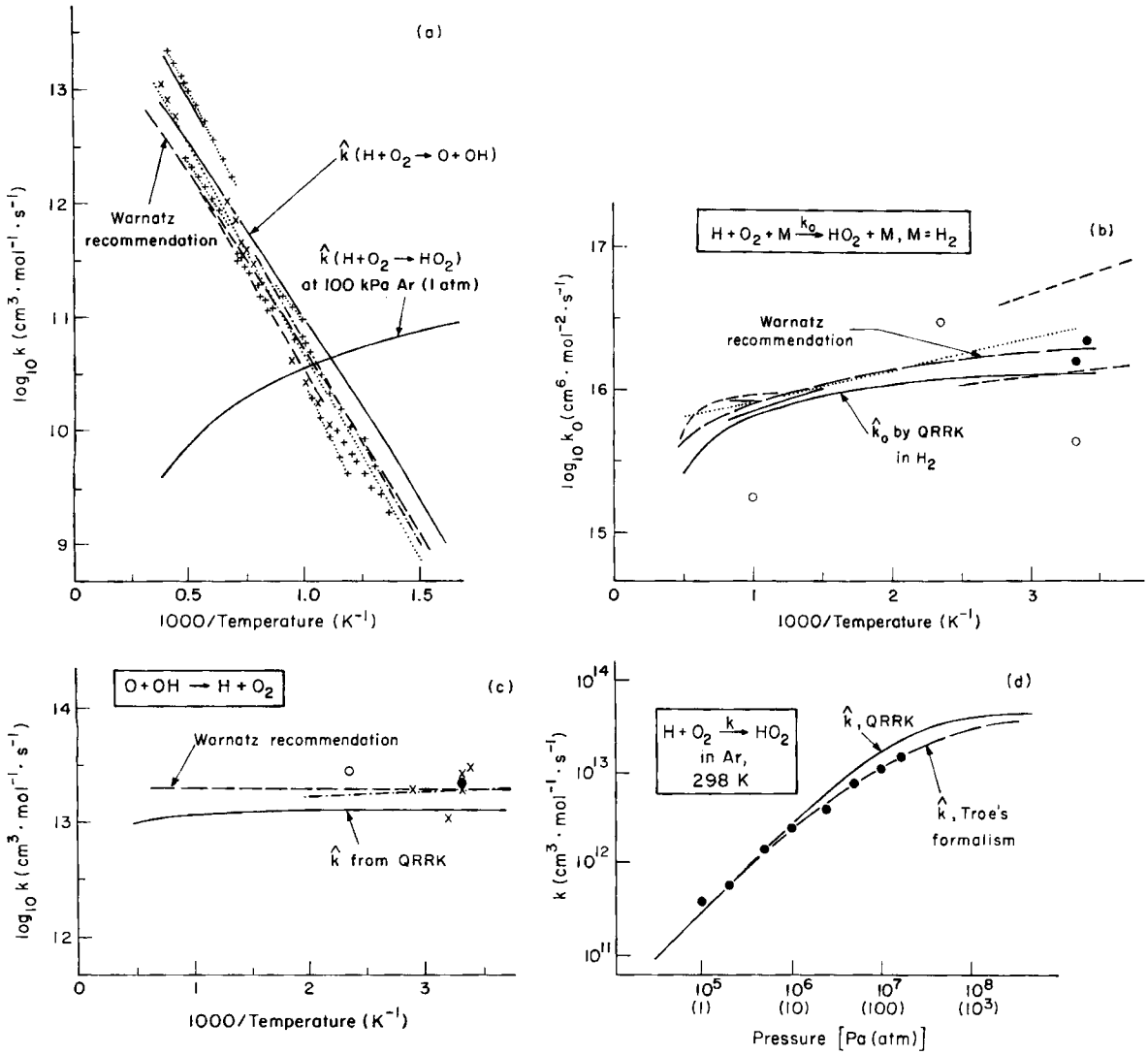

Figure 5. Comparison of QRRK predictions for rate constants in the system H + O_2/HO_2/O(^3P) + OH.

a. QRRK-predicted second-order rate constants (—) for indicated reactions compared to data of Warnatz (1984) for H + O_2 → O + OH reaction.

b. QRRK-predicted low-pressure limit k_o for indicated reaction compared to data of Warnatz (1984).

c. QRRK-predicted rate constant for indicated reaction compared to data of Warnatz (1984)

d. QRRK-predicted falloff curve for indicated reaction compared to data of Cobos et al. (1985a).

become pressure-dependent, but at 100 kPa (1 atm), it is in a chemical-activation low-pressure limit (Eq. 10). The predictions for HO_2 formation at 100 kPa are also shown, showing the change in branching that makes HO_2 chemistry important at lower temperatures and H + O_2 → O + OH important at higher temperatures. For k_o of H + O_2 + M → HO_2 + M (M = H_2) and $k_{a/d}$ of O + OH → H + O_2, Figures 5b and 5c, agreement is excellent. Predictions of the falloff curve for H + O_2 → HO_2 are compared to data in Figure 5d, showing agreement within a factor of two.

The k_∞ for O + OH → HO_2 was the only estimated parameter used in making these predictions. Of all the rate constants, only $k_{a/d}$ of O + OH → H + O_2 was sensitive to this estimate. In terms of Eq. 10, this rate constant was in a chemical-activation low-pressure limit with $k_{a/d} = 0.53 \cdot k_\infty$ (O + OH → HO_2) at 300 K. The purpose of this analysis was to test the method without adjusting parameters, but the slight disagreement between data and theory would be reconciled by setting k_∞ (O + OH) to $3.0 \cdot 10^{13}$.

Reactions of H + C_2H_4

C_2H_5 is produced as an intermediate by hydrogen abstraction or beta-scission of larger radicals during cracking processes to make ethylene. The radical then can decompose to H + C_2H_4 with a pressure-dependent rate constant. The reverse reaction, addition, is likewise important, and it competes with a pressure-independent abstraction reaction H + C_2H_4 → H_2 + C_2H_3. As noted before, falloff curves for decomposition and addition will be the same if there is no other decomposition channel involved.

To make predictions of the rate constant by bimolecular QRRK, k_∞ for addition and k for abstraction were taken from the recommendations of Warnatz (1984). High-pressure Arrhenius parameters for decomposition were calculated using the

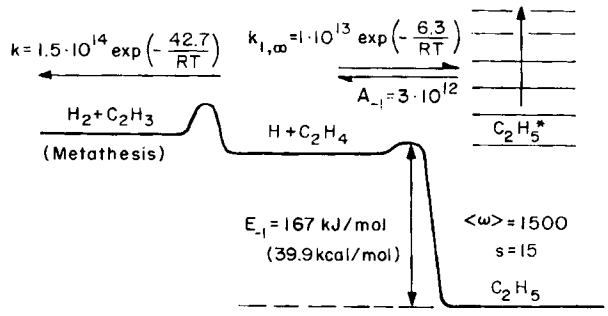

Figure 6. Energy diagram of H + C_2H_4 reactions.

equilibrium constant at 298 K, as before. The geometric mean frequency $\langle\omega\rangle$ for C_2H_5 is approximately 1,500 cm^{-1} with $\mathcal{L}$ = 15. Argon was assumed as the collision partner M. The parameters are summarized on the energy diagram of Figure 6.

In Figure 7a, predictions of the rate constant for addition are compared to the rate constant for the abstraction reaction that forms C_2H_3 + H_2. Addition dominates the branching between products at low temperatures, and abstraction dominates at high temperatures. Clearly, pressure determines the temperature at which abstraction becomes more important than addition.

The low-pressure limit for decomposition of C_2H_5 was calculated using the low-pressure limit for addition/stabilization and the equilibrium constant. Agreement with data is excellent, Figure 7b.

Reactions of H + C_2H_3

As a final example, the reaction of H-atom and vinyl radical was considered. Both species are important in pyrolysis and combustion. Formation of H_2 + C_2H_2 is reported with a high rate constant ($2.0 \cdot 10^{13}$), but data are rather scattered (Warnatz, 1984). The reaction has been attributed to H-transfer by radical-radical disproportionation, which is typically fast. This explanation seems unlikely because disproportionation has been rationalized (Benson, 1983) as being the product of long-range, polar interactions, which H cannot have.

Analysis of the rate constant by bimolecular QRRK showed that the data were described well by combination of H and C_2H_3 to form excited $C_2H_4^*$, decomposing to H_2 + C_2H_2 by a four-center molecular elimination. These steps correspond to the two product channels of H + C_2H_3 and H_2 + C_2H_2 that have been reported for C_2H_4 pyrolysis.

Input parameters are shown in Figure 8. The k_∞ for H + C_2H_3 was estimated by the recombination method used above for O + OH (Benson, 1983; Westmoreland, 1986). For the molecular elimination of H_2 from C_2H_4, $E_{act,\infty}$ has been estimated by Benson and Haugen (1966) as 339 kJ/mol (81 kcal/mol) at 1,500 K, and $\mathcal{A}_\infty$ has been calculated from their transition-state geometry (Westmoreland, 1986). For C_2H_4, $\mathcal{L}$ = 12 and $\langle\omega\rangle$ = 1586 cm^{-1} (Stull et al., 1972).

This analysis predicts the experimental rate constants well, Figure 9. Also, $k_{a/d}$ is predicted to be pressure-dependent at conditions of practical interest. Rate constants for 2.7 and 100 kPa are predicted to converge at high temperatures in a pressure-independent, low-pressure limit for chemical activation. However, at lower temperatures, only the 2.7 kPa rate constant is near the low-pressure limit.

The analysis is not a proof of mechanism, but it overcomes the

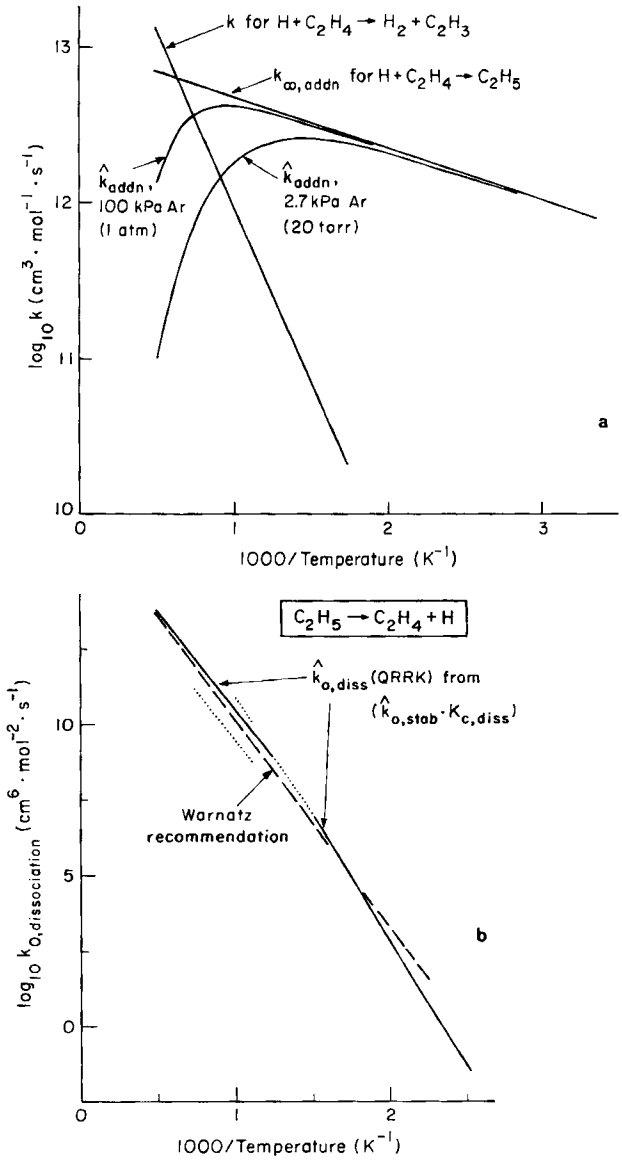

Figure 7. Comparisons of QRRK predictions for rate constants of H + C_2H_4 reactions.

a. Arrhenius plot for addition at 2.7, 100, and ∞ kPa in Ar. Abstraction reaction to H_2 + C_2H_3 also shown for reference.
b. k_o for C_2H_5 dissociation compared to data of Warnatz (1984).

difficulty of explaining a disproportionation involving H. No parameters were adjusted, and the only major uncertainty is the energy barrier for four-center elimination of H_2 from C_2H_4. A three-center elimination of H_2 has also been suggested to explain H_2 production from C_2H_4 pyrolysis, in which C_2H_4 would isomerize to CH_3CH (Bauer, 1967). To have a temperature-independent rate constant, either path would require an energy barrier less than that from C_2H_4 to H + C_2H_3.

Conclusions

A bimolecular adaptation of unimolecular QRRK (Kassel, 1928) by Dean (1985) is shown to predict correctly the pressure and temperature dependences of various reactions important to modeling combustion and pyrolysis. The reactions that can be

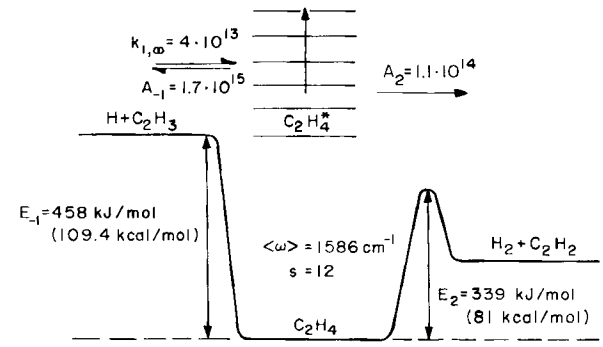

Figure 8. Energy diagram for H + C_2H_3 reactions.

treated are additions or combinations, which initially form excited intermediates. These excited species may be stabilized by collisions with surrounding molecules or may undergo energy-dependent unimolecular reactions such as decomposition. In contrast, H-atom transfer reactions pass through a single transition state to products, so they have pressure-independent rate constants.

Significantly, the intermediate is not thermalized or ground-state A, but it is rather a distribution of excited A^* states having a distribution of energies from E_{-1} (m_{-1}) above the ground state to ∞. Thus, $P + P'$ is formed directly and at a different rate than if it had been formed by the series of recombination and dissociation reactions $R + R' \rightarrow A \rightarrow P + P'$. Temperature dependence of the rate constants is strongly affected by the energy distribution $f(E, T)$, which spreads toward higher energy levels as temperature increases. Also, because A^* has energies of E_{-1} and above, new dissociation channels may become accessible, even though they might be unimportant steps for thermal decomposition of A.

The form of this method makes the problem and the results easier to apply and to understand. For example, low- and high-pressure limits for the rate constants are easily derived and interpreted. Some accuracy is sacrificed relative to the more complex methods, but the necessary data for QRRK are fewer and simpler. All input parameters are properties of the radical or molecule that is the stabilized adduct: collision properties, vibrational frequencies, and high-pressure-limit rate constants

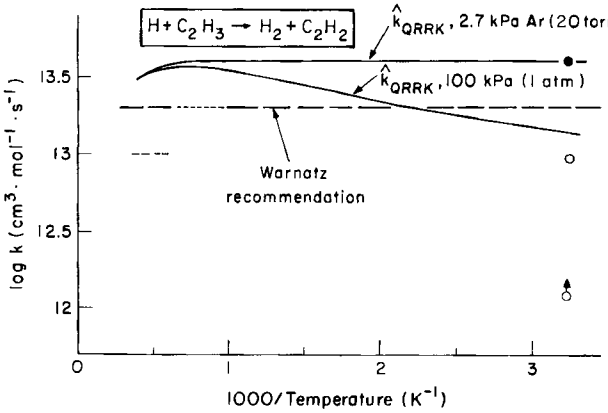

Figure 9. QRRK predictions for rate constants of indicated reaction compared with data of Warnatz (1984).

for its unimolecular reactions. Such parameters often are available in the literature or can be estimated with good accuracy.

For modeling combustion or pyrolysis, use of this method gives useful predictions of the effects of pressure on rate constants. The method's success with applications in this article show how it can be used to correlate data and to help the researcher understand the chemical mechanisms involved. Finally, by applying this technique, we can better estimate rate constants of reactions for which we have few or no measurements.

Input parameters for the above cases may be refined, particularly as better k_∞ data become available. For example, $k_\infty(C_2H_5 \rightarrow C_2H_4 + H) = 1.22 \cdot 10^{14} \exp(-167/RT)$, $k_\infty(C_2H_4 + H \rightarrow C_2H_5) = 2 \cdot 10^{14} \exp(-6.3/RT)$, $\langle\omega\rangle(C_2H_5) = 1458\ cm^{-1}$, and $k_\infty(C_2H_4 \rightarrow C_2H_2 + H_2) = 2.1 \cdot 10^{14} \exp(-372/RT)$ (Westmoreland, 1986) seem to be more accurate. Using these numbers, the conclusions above about the corresponding chemically activated reactions are not changed, and agreement with the data remains good or excellent.

Acknowledgment

We are grateful to Exxon Research and Engineering Company for financial support of this research through the EXXON-MIT Combustion Research Program.

Notation

$\mathcal{A}$ = Arrhenius preexponential factor
$\mathcal{A}_\infty$ = $\mathcal{A}$ in the high-pressure limit
c = velocity of light
E = energy content (variable) of adduct A
E_{act} = Arrhenius activation energy
$E_{act,\infty}$ = E_{act} in the high-pressure limit
E_o = energy barrier to unimolecular reaction
E_{-1} = barrier for dissociation of A to reactants
E_2 = barrier for dissociation of A to new products
$f(E, T)$ = energy distribution function for chemical activation
$F(E)$ = energy dependence factor of the density of states
h = Planck constant
$K(E, T)$ = thermal energy distribution function
$k_{a/s}$ = apparent rate constant for addition with stabilization
$k_{a/d}$ = apparent rate constant for addition with chemically activated decomposition of the excited adduct to new products
k_{bi} = observed bimolecular rate constant
k_{deexc} = rate constant for collisional stabilization
k_{exc} = rate constant for collisional excitation
k_{rxn} = rate constant for unimolecular reaction of A^*
k_{uni} = observed unimolecular rate constant
k_o = rate constant in the low-pressure limit
$k_{1,\infty}$ = rate constant for addition in the high-pressure limit
$k_{-1}(E)$ = rate constant for dissociation of $A^*(E)$ to reactants
$k_2(E)$ = rate constant for dissociation of $A^*(E)$ to products
k_∞ = rate constant in the high-pressure limit
m = quantized energy barrier to unimolecular reaction
n = quantized energy variable ($=E/h\langle\nu\rangle$)
n_{atoms} = number of atoms in a molecule
P = pressure
R = universal gas constant
s = number of vibrational degrees of freedom in species A
T = temperature
Z = collision frequency at unit concentration
Z_{LJ} = Z for Lennard-Jones interaction potentials

Greek letters

α = $\exp(-h\langle\nu\rangle/\kappa T)$
β = collision efficiency for energy removal
$\langle\Delta E_{coll}\rangle$ = average energy transferred per collision
ϵ = Lennard-Jones interaction energy

κ = Boltzmann constant
ν = frequency, s^{-1}
$\langle\nu\rangle$ = geometric-mean frequency of A
σ = Lennard-Jones collision diameter
$\langle\omega\rangle$ = geometric-mean frequency of A, cm^{-1}; $\nu = \omega \cdot c$

Literature Cited

Bauer, S. H., "Transient Species Generated during the Pyrolysis of Hydrocarbons," *11th Int. Symp. Combustion,* Combustion Inst., Pittsburgh, 105 (1967).

Baulch, D. L., D. D. Drysdale, J. Duxbury, and S. J. Grant, *Evaluated Kinetic Data for High Temperature Reactions, Vol. 3,* Butterworths, London (1976).

Berman, M. R., and M. C. Lin, "Kinetics and Mechanisms of the Reactions of CH and CD with H_2 and D_2," *J. Chem. Phys.,* **81,** 5743 (1984).

Benson, S. W., *Thermochemical Kinetics, 2nd Ed.,* Wiley (1976).

———, "Molecular Models for Recombination and Disproportionation of Radicals," *Can. J. Chem.,* **61,** 881 (1983).

Benson, S. W., and G. R. Haugen, "Estimated Activation Energies for the Four-Center Addition Reactions of H_2, HX, and X_2," *J. Phys. Chem.,* **70,** 3336 (1966).

Cobos, C. J., H. Hippler, and J. Troe, "High-Pressure Falloff Curves and Specific Rate Constants for the Reactions $H + O_2 \rightleftharpoons HO_2 \rightleftharpoons HO + O$," *J. Phys. Chem.,* **89,** 342 (1985a).

———, "Falloff Curves of the Recombination Reaction $O + SO + M \rightleftharpoons SO_2 + M$," *J. Phys. Chem.,* **89,** 1778 (1985b).

Dean, A. M., "Predictions of Pressure and Temperature Effects upon Radical Addition and Recombination Reactions," *J. Phys. Chem.,* **89,** 4600 (1985).

Forst, W., *Theory of Unimolecular Reactions,* Academic Press, New York (1973).

Gardiner, W. C., Jr., and J. Troe, "Rate Coefficients of Thermal Dissociation, Isomerization, and Recombination Reactions," *Combustion Chemistry,* (W. C. Gardiner, Jr., ed.), Springer-Verlag, New York (1984).

Howard, C. J., "Kinetic Study of the Equilibrium $HO_2 + NO \rightleftharpoons OH + NO_2$ and the Thermochemistry of HO_2," *J. Am. Chem. Soc.,* **102,** 6937 (1980).

Kassel, L. S., "Studies in Homogeneous Gas Reactions II. Introduction of Quantum Theory," *J. Phys. Chem.,* **32,** 1065 (1928).

Kee, R. J., J. Warnatz, and J. A. Miller, "A Fortran Computer Code Package for the Evaluation of Gas-phase Viscosities, Conductivities, and Diffusion Coefficients," Sandia Lab. Rept. SAND83-8209, Livermore, CA (1983).

Pritchard, H. O., *The Quantum Theory of Unimolecular Reactions,* Cambridge University Press, Cambridge (1984).

Reid, R. C., J. M. Prausnitz, and T. K. Sherwood, *The Properties of Gases and Liquids, 3rd Ed.,* McGraw-Hill, New York (1977).

Robinson, P. J., and K. A. Holbrook, *Unimolecular Reactions,* Wiley-Interscience, London (1972).

Stull, D. R., H. Prophet, et al., *JANAF Thermochemical Tables, 2nd Ed.,* Nat. Bur. Standards, Washington, DC, NSRDS-NBS 37 (1971).

Thiele, E., J. Stone, and M. F. Goodman, "On the Use of Geometric or Arithmetic Mean Frequency in Quantum RRK Theory," *Chem. Phys. Letters,* **76,** 579 (1980).

Troe, J., "Thermal Dissociation and Recombination of Polyatomic Molecules," *15th Int. Symp. Combustion,* The Combustion Inst., Pittsburgh, 667 (1974).

———, "Theory of Thermal Unimolecular Reactions at Low Pressures. I. Solutions of the Master Equation. II. Strong Collision Rate Constants. Applications," *J. Chem. Phys.,* **66,** 4745 and 4758 (1977).

———, "Predictive Possibilities of Unimolecular Reaction Rate Theory," *J. Phys. Chem.,* **83,** 114 (1979).

Warnatz, J., "Rate Coefficients in the C/H/O System," *Combustion Chemistry,* (W. C. Gardiner, Jr., ed.), Springer-Verlag, New York (1984).

Westmoreland, P. R., *Experimental and Theoretical Analysis of Oxidation and Growth Chemistry in a Fuel-Rich Acetylene Flame,* Ph. D. diss., Dept. of Chem. Eng., Massachusetts Inst. of Tech. (1986).

Manuscript received Oct. 18, 1985, and revision received April 4, 1986.